

# Dalton Transactions

Accepted Manuscript



This is an *Accepted Manuscript*, which has been through the Royal Society of Chemistry peer review process and has been accepted for publication.

*Accepted Manuscripts* are published online shortly after acceptance, before technical editing, formatting and proof reading. Using this free service, authors can make their results available to the community, in citable form, before we publish the edited article. We will replace this *Accepted Manuscript* with the edited and formatted *Advance Article* as soon as it is available.

You can find more information about *Accepted Manuscripts* in the [Information for Authors](#).

Please note that technical editing may introduce minor changes to the text and/or graphics, which may alter content. The journal's standard [Terms & Conditions](#) and the [Ethical guidelines](#) still apply. In no event shall the Royal Society of Chemistry be held responsible for any errors or omissions in this *Accepted Manuscript* or any consequences arising from the use of any information it contains.

# Distinguishable Zn(II) and Pb(II) template effects on forming pendant-armed Schiff-base macrocyclic complexes including a remarkable Pb(II)- $\pi$ macrocyclic complex

Cite this: DOI: 10.1039/x0xx00000x

Received 00th June 2014,  
Accepted 00th 2014

DOI: 10.1039/x0xx00000x

www.rsc.org/dalton

Kun Zhang,<sup>a</sup> Jiao Geng,<sup>a</sup> Chao Jin<sup>b</sup> and Wei Huang<sup>\*a</sup>

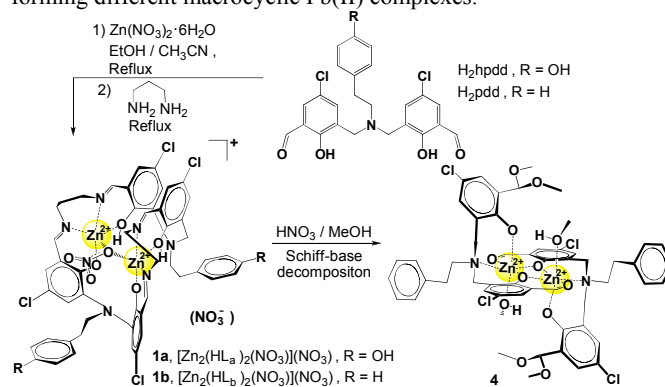
36-Membered [2+2] half-fold Schiff-base macrocyclic dinuclear Zn(II) complexes (**1a** and **1b**) and 18-membered [1+1] Schiff-base macrocyclic mononuclear Pb(II) complexes (**2** and **3**) are produced from the condensation between 1,3-propanediamine and a pair of extended dialdehydes with different functional pendant arms (H<sub>2</sub>hpdd and H<sub>2</sub>pdd) because of the distinguishing cationic template effects. It is very interesting to mention that a unique intramolecular Pb(II)- $\pi$  macrocyclic complex **2** with an uncommon  $\eta^3$ -coordinated type is achieved under ambient condition and it can keep stable both in the solid state and in solution. The subtle variations of pendant-arms in the macrocyclic ligands H<sub>2</sub>hpdd and H<sub>2</sub>pdd yield different Pb(II) complexes, where the competition between Pb(II)- $\pi$  and Pb(II)-NO<sub>3</sub><sup>-</sup> electrostatic interactions as well as the combination of steric and electronic effects of pendant arms is believed to play important roles.

## Introduction

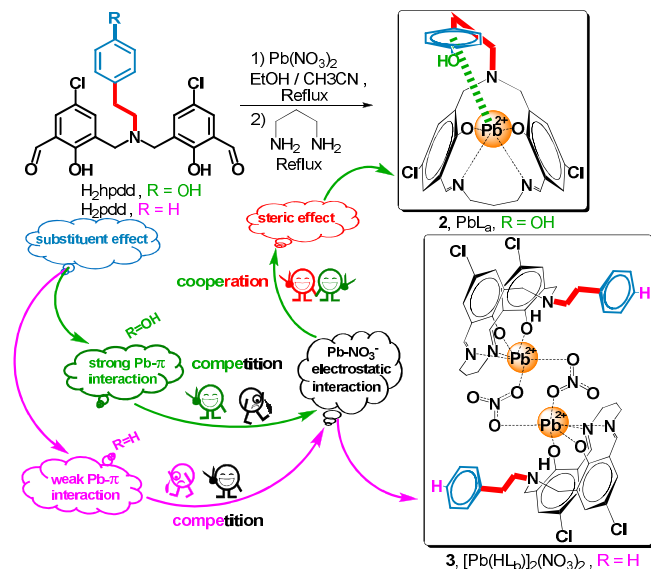
As one of the most important fields in macrocyclic and supramolecular chemistry, Schiff-base macrocycles have been widely and deeply studied involving relative syntheses, characterizations, properties and applications.<sup>1</sup> But so far, it is still a challenge to synthesize a new Schiff-base macrocycle for the complexity of multiple Schiff-base condensation between the dicarbonyl compounds and diamines. During the past four decades, considerable efforts have been made to develop metal-free and metal-template<sup>2</sup> methods for imagined macrocycles. Commonly, the strategy of metal-template method is more effective to cyclise, and this method could control the size of Schiff-base macrocycles by different metal template ions. The reason is the final macrocyclic ligands should match the size, charge and optimal coordination geometry of the metal template ion.

Our continuous interest in the Schiff-base macrocycles<sup>3</sup> leads us to explore the construction of Schiff-base macrocycles with alterable size by using the same dialdehydes and diamines but different metal template ion. In this work, two flexible extended dialdehydes (H<sub>2</sub>hpdd and H<sub>2</sub>pdd) with different functional pendant arms (-CH<sub>2</sub>CH<sub>2</sub>PhOH and -CH<sub>2</sub>CH<sub>2</sub>Ph)<sup>3d</sup> as well as 1,3-propanediamine have been used to build metallomacrocycles with alterable size in the presence of suitable metal template ions. As a result, two 36-membered [2+2] half-fold macrocyclic dinuclear Zn(II) complexes **1a** and **1b** (Scheme 1) and two 18-membered [1+1] macrocyclic mononuclear Pb(II) complexes **2** and **3** (Scheme 2) are produced,

respectively, because of the distinguishing Zn(II) and Pb(II) metal template effects, which are different from the formation of identical [2+2] dinuclear Zn(II) and Pb(II) macrocyclic complexes by using 2,6-diformoyl-4-chlorophenol as a dialdehyde precursor.<sup>3a,4c</sup> At the same time, it is worthwhile to mention that a unique Pb(II)- $\pi$  interaction is observed under ambient condition, where the subtle variations of pendant-arms of macrocyclic ligands yield different products. The competition between Pb(II)- $\pi$  and Pb(II)-NO<sub>3</sub><sup>-</sup> electrostatic interactions as well as the combination of steric and electronic effects of pendant arms are believed to play vital roles in forming different macrocyclic Pb(II) complexes.



**Scheme 1.** Synthetic route for the 36-membered [2+2] half-fold Schiff-base macrocyclic dinuclear Zn(II) complexes **1a** and **1b** as well as the dinuclear Zn(II) decomposition product **4**.



**Scheme 2.** Schematic illustration for the competition between  $\text{Pb}(\text{II})-\pi$  and  $\text{Pb}(\text{II})-\text{NO}_3^-$  electrostatic interactions as well as the combination of steric and electronic effects of pendant arms in forming distinguishable 18-membered [1+1] macrocyclic mononuclear  $\text{Pb}(\text{II})$  complexes.

Further pH stability investigations reveal that  $\text{Pb}(\text{II})$  macrocyclic complexes can keep stable in the pH range of 5–8. In contrast,  $\text{Zn}(\text{II})$  macrocyclic complexes underwent Schiff-base decomposition by adding either acid or base. As a result, a dinuclear  $\text{Zn}(\text{II})$  decomposition complex **4** was obtained in the acidic condition ( $\text{pH} = 3\sim 4$ ) after the addition of  $0.05 \text{ mol/L}^{-1} \text{ HNO}_3$  into the methanol solution of  $\text{Zn}(\text{II})$  macrocyclic complex **1b** (Scheme 1), where a dimethylacetalization reaction occurred for half of the aldehyde groups of pdd divalent anions.

## Results and discussion

### Syntheses

In the synthesis of Schiff-base macrocyclic metal complexes, metal template effects are critical. In this respect, the importance of metal template ions is reflected in directing the course of multiple Schiff-base condensation to macrocycles and increasing the yields of macrocyclic products. As is reported, all the Schiff-base condensation between 2,6-diformyl-4-substituted phenol and 1,3-propanediamine in the presence of many transition-metal ions ( $\text{Mn}$ ,  $\text{Fe}$ ,  $\text{Co}$ ,  $\text{Ni}$ ,  $\text{Cu}$ ,  $\text{Zn}$ ,  $\text{Cd}$ ,  $\text{Pb}$ ,  $\text{Pd}$ ) produces [2+2] macrocyclic dinuclear complexes.<sup>4</sup> The same type of ultimate metal macrocyclic products is due to the compromise between the size, charge and coordination geometry of metal template ions together with the flexibility of macrocyclic skeleton. However, our results in this work demonstrate that the treatment of extended dialdehydes ( $\text{H}_2\text{hpdd}$  and  $\text{H}_2\text{pdd}$ ) and 1,3-propanediamine in the presence of  $\text{Zn}(\text{NO}_3)_2 \cdot 6\text{H}_2\text{O}$  and  $\text{Pb}(\text{NO}_3)_2$  will yield distinguishable 36-membered [2+2] half-fold macrocyclic dinuclear  $\text{Zn}(\text{II})$  complexes (Scheme 1) and 18-membered [1+1] macrocyclic mononuclear  $\text{Pb}(\text{II})$

template effects is still expressed on forming flexible Schiff-base macrocyclic skeleton based on flexible dialdehyde and diamine.

It should be pointed out that all the Schiff-base macrocyclic  $\text{Zn}(\text{II})$  and  $\text{Pb}(\text{II})$  complexes in this paper are obtained in weak acidic condition with pH value about 5–6. Finally, half of the phenolic protons are removed in dinuclear  $\text{Zn}(\text{II})$  complexes **1a** and **1b** and [1+1]  $\text{Pb}(\text{II})$  complex **3**. However, all the phenolic protons are removed with regard to the [1+1]  $\text{Pb}(\text{II})-\pi$  complex **2**. Considering that different amounts of phenolic protons are present in these macrocyclic complexes, pH stability investigations have been carried out by adding  $0.05 \text{ mol/L}^{-1} \text{ HNO}_3$  and  $\text{NaOH}$  before and after the formation of metallomacrocycles, respectively. Our results indicate that no macrocyclic compounds could be yielded if acid or base was added before the Schiff-base condensation. When complexes **1–3** were treated with acid or base, two  $\text{Zn}(\text{II})$  complexes decomposed quickly accompanied by the appearance of precipitates, and a dinuclear  $\text{Zn}(\text{II})$  complex **4** was obtained in the acidic condition after the addition of  $0.05 \text{ mol/L}^{-1} \text{ HNO}_3$  into the methanol solution of  $\text{Zn}(\text{II})$  macrocyclic complex **1b**. However, two  $\text{Pb}(\text{II})$  complexes are found to be stable in the pH range of 5–8, and precipitates will also be formed outside this pH range.

Interestingly, a unique  $\text{Pb}(\text{II})-\pi$  macrocyclic complex is achieved under ambient condition, where the subtle variations of pendant arms of macrocyclic ligands yield different products of **2** and **3**, as illustrated in Scheme 2. The competition between  $\text{Pb}(\text{II})-\pi$  and  $\text{Pb}(\text{II})-\text{NO}_3^-$  electrostatic interactions as well as the combination of steric and electronic effects of pendant arms is believed to play vital roles in forming different macrocyclic  $\text{Pb}(\text{II})$  complexes.

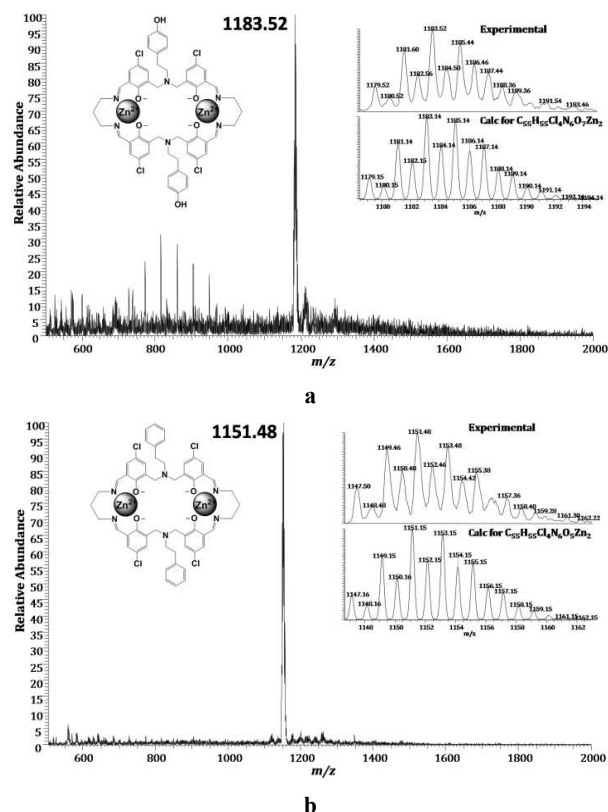


**Figure 1.** Positive ESI-MS of 36-membered [2+2] macrocyclic dinuclear  $\text{Zn}(\text{II})$  complexes **1a** (a) and **1b** (b) obtained in the positive

mode, together with the experimental and calculated IDPs (Inset) corresponding to the peak at 100% abundance for comparison.

### Spectral Characterizations

Relative spectral analyses are used to monitor this type of Schiff-base cyclization. From previous work,<sup>3d</sup> it is known that the FT-IR absorption peak of aldehyde groups is found to be 1660 and 1664  $\text{cm}^{-1}$  in  $\text{H}_2\text{hpdd}$  and  $\text{H}_2\text{pdd}$ , respectively. In contrast, a new absorption peak is observed at 1639 and 1632  $\text{cm}^{-1}$  in **1a** and **1b** and 1634  $\text{cm}^{-1}$  in **2** and **3** replacing the peak of aldehyde groups, indicative of the formation of C=N Schiff-base units. From the ESI-MS spectra of **1a** and **1b**, the formation of 36-membered [2+2] macrocyclic dinuclear Zn(II) complexes can be proven by a positive peak at  $m/z = 1183.52$  and 1151.48 (Figure 1), respectively, corresponding to the species of  $\{[\text{Zn}_2(\text{L}_a)_2] + \text{CH}_3\text{OH} + \text{H}\}^+$  and  $\{[\text{Zn}_2(\text{L}_b)_2] + \text{CH}_3\text{OH} + \text{H}\}^+$ , which agrees well with the theoretic simulations.

Furthermore,  $^1\text{H}$  NMR spectral characterization have been carried out to explore the variations of chemical shifts between dialdehyde precursors and their relative Zn(II) and Pb(II) macrocyclic complexes. New peaks are observed at 7.93 ppm in **1a** ( $\text{CD}_3\text{OD}$ ), 7.97–8.24 ppm in **1b** ( $\text{CD}_3\text{CN}$ ), and 8.18 ppm in **2** and **3** ( $\text{CD}_3\text{OD}$ ), assigned as the formation of imine units. In order to further explore the Pb(II)- $\pi$  interactions in solution, the comparisons among the  $^1\text{H}$  NMR spectra have been carried out for  $\text{H}_2\text{hpdd}$ ,  $\text{H}_2\text{pdd}$ , and their respective Pb(II) complexes **2** and **3** in  $\text{CD}_3\text{OD}$ . As displayed in Figure 2, the aromatic protons of two *p*-Cl-phenol rings in **2** and **3** are shifted to the higher field (the green ones), mainly because the deprotonation and subsequent increase of electron density are overwhelming compared with the Pb(II) ion complexation induced deshielding effects. It is noted that three pairs of protons are found to have the same  $\delta$  values in **2** and **3**, i.e., 8.18 ppm (7 and 11) for the Schiff-base units and 7.08 ppm (5 and 13) and 6.97 ppm (3 and 15) for the two *p*-Cl-phenol hydrogen atoms, indicative of the formation of the same macrocyclic backbone.

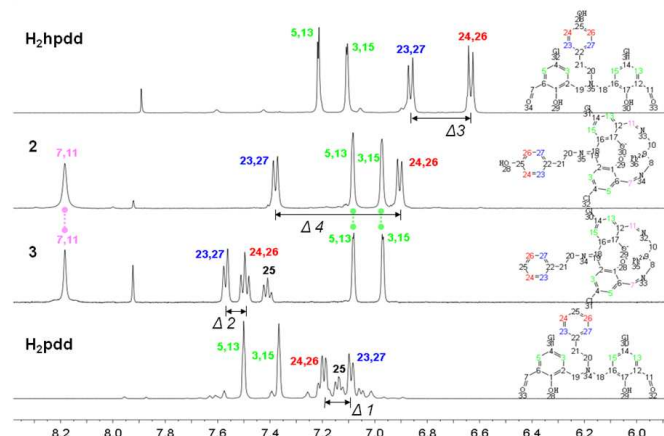


**Figure 2.**  $^1\text{H}$  NMR spectral comparisons of extended dialdehydes and their [1+1] macrocyclic Pb(II) complexes **2** and **3** in the low field in  $\text{CD}_3\text{OD}$ , together with the assignments for the chemical shifts of protons.

However, the four aromatic protons of the pendant arms in **2** and **3** are significantly shifted to the lower field (ca. 0.2–0.5 ppm) after

Pb(II) ion complexation, and they can be divided into two groups shown as blue (23 and 27) and red (24 and 26), respectively. Here, a parameter  $\Delta$ , namely the chemical shift difference for two groups of protons, is defined. By comparing  $\Delta_1$  (0.10 ppm) and  $\Delta_2$  (0.07 ppm) in  $\text{H}_2\text{pdd}$  and **3** with  $\Delta_3$  (0.23 ppm) and  $\Delta_4$  (0.47 ppm) in  $\text{H}_2\text{hpdd}$  and **2**, as illustrated in Figure 2, it is found that two pairs of aromatic protons in the latter show distinguishable chemical environments after Pb(II) ion complexation, indicating the existence of Pb(II)- $\pi$  interaction in solution. Furthermore, a large chemical shift difference of  $\Delta_4$  reveals the formation of afore-mentioned  $\eta^3$ -coordinated mode in **2**, which means that the Pb lone-pair donates to the  $\pi^*$  orbital of the phenolic ring in the pendant arm, mainly the carbon atoms of C25, C26 and C27. In contrast, small  $\Delta$  values observed in the former pair reveal the absence of Pb(II)- $\pi$  interaction in solution. So it is concluded that the  $^1\text{H}$  NMR spectral comparisons before and after metal-ion complexation provide an experimental proof on the stable existence of Pb(II)- $\pi$  interactions in solution in the case of complex **2**, and a  $\eta^3$ -coordinated mode is detected between the phenolic ring and the Pb(II) center agreeing well with the following structural description.

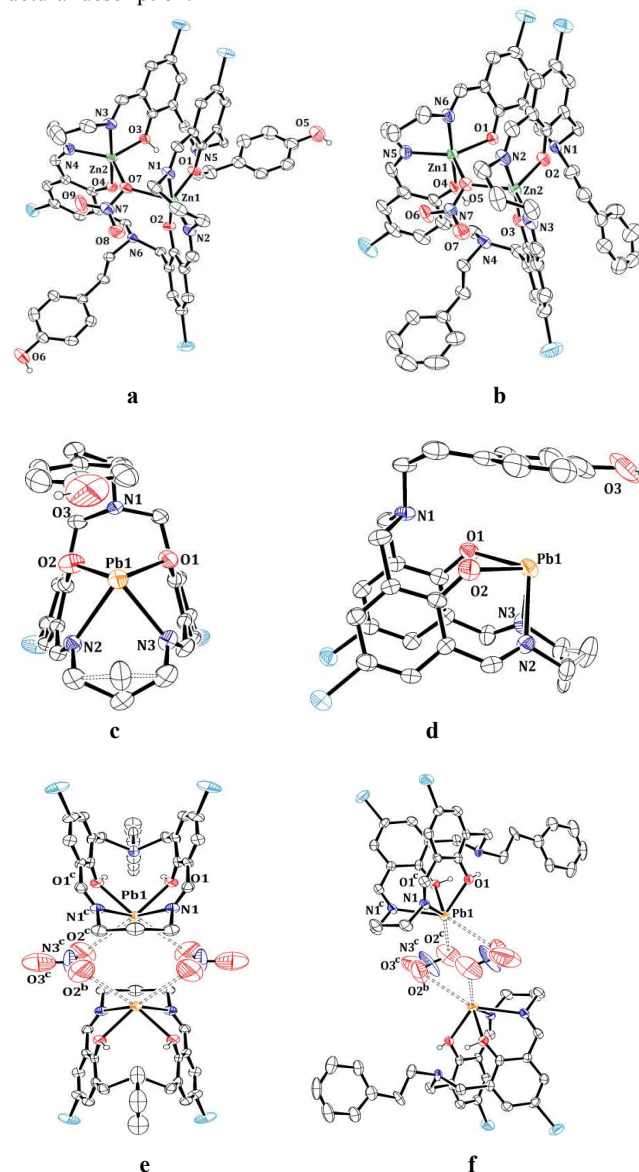


**Figure 3.** ORTEP drawings of Zn(II) complexes, **1a** (a) and **1b** (b), and Pb(II) complexes, **2** (c and d) and **3** (e and f), with the atom-numbering scheme. Displacement ellipsoids are drawn at the 30 % probability level and the phenolic protons are shown as small spheres of arbitrary radii. The counterion, solvent and hydrogen atoms except the phenolic protons are omitted for clarity,

### Crystal Structures

**Structures of 1a and 1b.** The molecule structures of **1a** and **1b** with the atom-numbering scheme are illustrated in Figures 2a and 2b, respectively. They are both 36-membered [2+2] half-fold macrocyclic dinuclear Zn(II) complexes where the coordination configuration for each five-coordinate zinc(II) center in **1a** and **1b** is distorted trigonal bipyramidal ( $\tau = 0.764, 0.842$  and  $0.981, 0.807$  for Zn1 and Zn2 in **1a** and **1b**).<sup>5</sup> There are two nitrate counterions in the asymmetric unit for each Zn(II) complex. One serves as a  $\mu_2$  linker where one oxygen atom is found to connect two neighboring Zn(II) ions with a Zn...Zn separation of 3.809(1) Å in **1a** and 3.792(4) Å in **1b**, while the other is free of the formation of coordinative bond. The basal coordination plane of each Zn(II) ion is composed of two oxygen and two nitrogen atoms of macrocyclic ligand as well as one common oxygen atom of the nitrite anion. It is noted that the dihedral angles between the phenol rings of two pendant arms are 6.9(2)° in **1a** and 63.3(2)° in **1b**. As for the half-fold macrocyclic ligands in **1a** and **1b**, the distances between the two *ortho* carbon atoms of each phenolic hydroxyl group for the extended part are 4.983(6) Å in **1a** and 4.952(4) Å in **1b**, which are longer than that in the free H<sub>2</sub>hpdd ligand (4.333(4) Å). In contrast, the folded units have the corresponding C...C separations of 3.064(6) Å in **1a** and 2.962(4) Å in **1b**. Additionally, intramolecular  $\pi$ - $\pi$  stacking interactions are observed between two adjacent facing 4-chlorophenol rings with the centroid-to-centroid separations of 3.480(1) Å in **1a** and 3.496(2) and 3.560(2) in **1b**.

**Structures of 2 and 3.** Different from the 36-membered [2+2] macrocyclic Schiff-base dinuclear compounds for Zn(II) ion template, 18-membered [1+1] macrocyclic mononuclear Pb(II) complexes **2** and **3** are produced for the same reaction when Pb(II) ion template is used. ORTEP drawings of **2** in Figures 2c-2d and **3** in Figures 2e-2f with the atom-numbering scheme are shown, where two oxygen and two nitrogen donors from the macrocyclic framework occupy half of the coordination sphere of Pb(II) ion with the Pb-O and Pb-N bond lengths in the ranges of 2.283(4)–2.330(8) Å and 2.462(5)–2.519(5) Å, respectively. However, it is worthwhile to mention that the subtle variations of pendant-arms (-CH<sub>2</sub>CH<sub>2</sub>PhOH vs. -CH<sub>2</sub>CH<sub>2</sub>Ph) of macrocyclic ligands yield different products because of the afore-mentioned competition between Pb(II)- $\pi$  and Pb(II)-NO<sub>3</sub><sup>-</sup> electrostatic interactions as well as the combination of steric and electronic effects of pendant arms. As a result, a unique Pb(II)- $\pi$  complex **2** is formed where the phenolic unit occupies the other half of the coordination sphere of central Pb(II) ion. In contrast, two NO<sub>3</sub><sup>-</sup> anions act as  $\mu_2$  bridges linking adjacent two mononuclear Pb(II) units by weak Pb-O coordinative bonds, where two oxygen atoms of each NO<sub>3</sub><sup>-</sup> anion are coordinated to the Pb(II) centers with the same bond length of 3.291(14) Å forming another dinuclear Pb(II) complex **3** mainly predominated by the Pb(II)-NO<sub>3</sub><sup>-</sup> electrostatic interactions.

The phenolic and phenyl rings of pendant arms in the macrocyclic ligands are found to point to different directions in **2** and **3** due to the

presence and absence of Pb(II)- $\pi$  interactions, and the related torsion angles (two alkyl carbon and two phenyl carbon atoms in the pendant arms) are 150.6(8)° in **2** and 0.0(3)° in **3**, respectively. In addition, intramolecular  $\pi$ - $\pi$  stacking interactions are observed between two facing 4-chlorophenol rings with the centroid-to-centroid separations of 3.767(11) Å in **2** and 3.916(11) Å in **3**, where the bite angles between the two 4-chlorophenol rings are 30.6(3)° in **2** and 34.4(3)° in **3**.

The Pb- $\pi$  interactions have been systematically summarized by Tiekink and Zukerman-Schpector in 2010,<sup>6c</sup> where 29 known examples having at least one aryl ring are involved. They proposed two geometric parameters: one is the distance ( $d$ ) between the centroid of the aryl ring and the lead center, and the other is the angle ( $\alpha$ ) defined by the vector perpendicular to the aryl ring ( $V_1$ ) and the vector passing through the ring centroid to the lead atom ( $V_2$ ), as described in Figure 5. They concluded that a Pb(II)- $\pi$  interaction should be considered as existence commonly if  $d < 4.0$  Å and  $\alpha < 20^\circ$ , and most of them fall within the ranges of  $2.78 < d < 3.97$  Å and  $0.6 < \alpha < 19.4^\circ$ . In our case, the two values are  $d = 3.549(1)$  Å and  $\alpha = 14.7(4)^\circ$ , which means that the Pb(II)- $\pi$  interaction does exist and it is a much weak one.

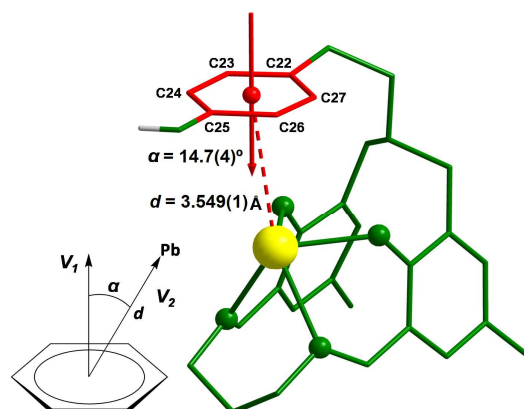


**Figure 4.** Illustration of the Pb(II)- $\pi$  interaction in complex **2** defined by two geometric parameters.

Further investigations on six Pb-C bond lengths in complex **2** indicate that they span a wide range from 3.468(10) to 4.102(8) Å, which is not a common  $\eta^6$ -coordinated mode. Instead, they adopt an intramolecular  $\eta^3$ -coordinated type where the three Pb-C (C25-C27) bond lengths are 3.708(10), 3.468(10), and 3.578(8) Å. In contrast, the other three Pb-C (C22-C24) bond lengths are much longer in the range of 3.946(7)–4.102(8) Å. This  $\eta^3$ -coordinated type for the Pb(II)- $\pi$  interaction observed in the solid state agrees well with the afore-mentioned <sup>1</sup>H NMR spectral results in solution.

Why we think this Pb(II)- $\pi$  macrocyclic complex **2** is structurally unique? Firstly, it provides a nice small molecular model compound containing the intramolecular Pb(II)- $\pi$  interaction. As a non-covalent bonding interaction, Pb- $\pi$  interaction is generally recognized as a supramolecular contact. A detailed analysis for Pb(II)- $\pi$  interactions by checking CCDC database shows that such a supramolecular interaction is not unusual.<sup>6</sup> However, most of them are related to the intermolecular Pb(II)- $\pi$  interactions within the supramolecular aggregates. In contrast, very few examples of Pb(II)- $\pi$  interactions are involved in the synthetic small molecules to date.<sup>6a</sup> Obviously, intramolecular Pb(II)- $\pi$  interaction between a neutral Pb(II) center

capped by a [1+1] macrocyclic ligand and its adjunctive phenol ring in complex **2** gives such a small molecular instance for further synthetic and theoretical investigations. In addition, complex **2** is stable in solution, which can be proven by the  $^1\text{H}$  NMR experiments. This phenomenon is different from the intermolecular  $\text{Pb(II)}-\pi$  complexes since solvation in solution usually leads to extensive disintegration of the molecular or multidimensional aggregates into the solvated components.<sup>6b</sup>

Secondly, study on the electron effects of the aromatic rings for  $\text{Pb(II)}-\pi$  interaction is realized once again by introducing different functional pendant arms. In general,  $\text{Pb(II)}-\pi$  interactions should be stronger and more prevalent if the electron density of the aromatic rings is increased, which may originate from the nature as donation of  $\pi$  electrons from the aromatic ring to vacant orbital of the Pb center.<sup>6b</sup> In our case, the only difference between complexes **2** and **3** is the substituted groups in the pendant arms ( $-\text{CH}_2\text{CH}_2\text{PhOH}$  vs.  $-\text{CH}_2\text{CH}_2\text{Ph}$ ). The former arm has higher electron density, which favors to form the  $\text{Pb(II)}-\pi$  complex. Fortunately, the single-crystal structures of  $\text{Pb(II)}$  complexes **2** and **3** have been obtained, clearly supporting the afore-mentioned viewpoint. The  $\text{Pb(II)}-\pi$  macrocyclic complex **2** adopts an extraordinary  $\eta^3$ -coordinated type. In contrast, most of reported  $\text{Pb(II)}-\pi$  interactions are described as the  $\eta^6$ -coordinated type in literature.<sup>6b,6c</sup> Nevertheless, the formation of intramolecular  $\text{Pb(II)}-\pi$  interaction in complex **2** is greatly restricted by the spatial crowding effects of two methane units in the pendant arm and the skeleton of macrocyclic ligand. So the final  $\eta^3$ -coordinated type is suggested to be a cooperative result of steric effect and  $\text{Pb(II)}-\pi$  interaction, which could be further verified by the following  $^1\text{H}$  NMR spectral and single-crystal structural investigations.

Thirdly, visual examples of  $\text{Pb(II)}$  macrocyclic complexes **2** and **3** are presented embodying the important role of anions. With regard to the factors involved in the formation of metal ion-aromatic complexes, Amma *et al.* proposed that the presence of a strong acid anion is vital in order to decrease the anion-cation binding, which will allow the appearance of metal- $\pi$  interaction.<sup>6m</sup> Herein  $\text{NO}_3^-$  is used as a counterion and the competition between  $\text{Pb(II)}-\pi$  and  $\text{Pb(II)}-\text{NO}_3^-$  electrostatic interactions is experimentally verified, where the  $\text{Pb(II)}-\pi$  interaction overwhelms the  $\text{Pb(II)}-\text{NO}_3^-$  electrostatic interaction in **2** and it is just the opposite in **3**. As a result, an intramolecular  $\text{Pb(II)}-\pi$  complex **2** against a dimer nitrate-bridged dinuclear  $\text{Pb(II)}$  complex **3** are obtained.

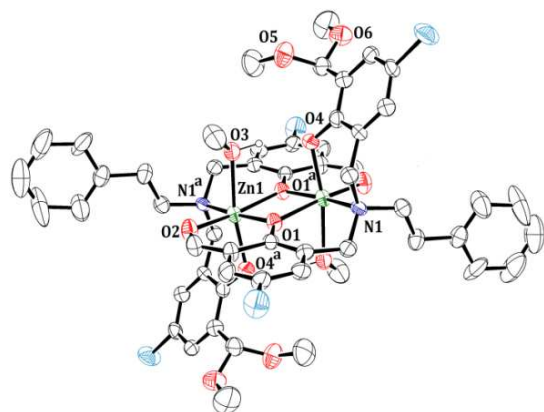


**Figure 5.** ORTEP drawing of  $\text{Zn(II)}$  complex **4** with the atom-numbering scheme. Displacement ellipsoids are drawn at the 30 %

probability level and all hydrogen atoms are omitted except the protons of coordinated methanol molecules.

**Structure of 4.** X-ray structural analysis of dinuclear  $\text{Zn(II)}$  intermediate **4** reveals that it is only composed of two pendant-armed dialdehyde components and two  $\text{Zn(II)}$  ions, where diamine units are removed because of the protonation of nitrogen atoms (Figure 5). The coordination geometry for each  $\text{Zn(II)}$  centre is a distorted six-coordinate octahedron. However, half of the aldehyde groups underwent a dimethylacetalization reaction with solvent methanol molecules. The resultant divalent anions act as a tetradentate ligand where two phenolic oxygen atoms, one aldehyde oxygen atom and the tertiary nitrogen atom are coordinated to the central  $\text{Zn(II)}$  ions. Two  $\mu_2$  phenolic oxygen atoms from each dialdehyde unit are found to link adjacent two  $\text{Zn(II)}$  ions, and the separation between them is 3.202(2) Å. In addition, two methanol molecules are coordinated to each  $\text{Zn(II)}$  ion to fill the rest of coordination sphere. The dihedral angles between the pendant-armed phenol ring and two salicylaldehyde rings in **4** are 71.8(5) and 80.9(4)°, respectively.

## Conclusion

In summary, 1,3-propanediamine is used to react with a pair of flexible extended dialdehydes with different functional pendant arms for Schiff-base macrocyclic complexes in the presence of  $\text{Zn(II)}$  and  $\text{Pb(II)}$  ion templates for comparison. As a result, 36-membered [2+2] half-fold macrocyclic dinuclear  $\text{Zn(II)}$  complexes (**1a** and **1b**) and 18-membered [1+1] macrocyclic mononuclear  $\text{Pb(II)}$  complexes (**2** and **3**) are produced, respectively, because of the distinguishing cationic template effects. FT-IR, ESI-MS and  $^1\text{H}$  NMR spectral and single-crystal structural methods are used to characterize their molecular structures.

It is very interesting to mention that a remarkable intramolecular  $\text{Pb(II)}-\pi$  interaction is found in macrocyclic complex **2** with an uncommon  $\eta^3$ -coordinated type is achieved under ambient condition, and it can keep stable both in the solid state and in solution, which can be clearly verified by its X-ray single-crystal structure and  $^1\text{H}$  NMR spectrum, in comparison with a similar  $\text{Pb(II)}$  macrocyclic complex **3** without the  $\text{Pb(II)}-\pi$  interactions. In this case, the subtle variations of pendant-arms in the macrocyclic ligands  $\text{H}_2\text{hpdd}$  and  $\text{H}_2\text{pdd}$  yield different  $\text{Pb(II)}$  complexes **2** and **3**, where the competition between  $\text{Pb(II)}-\pi$  and  $\text{Pb(II)}-\text{NO}_3^-$  electrostatic interactions as well as the combination of steric and electronic effects of pendant arms is believed to play vital roles. It is believed that the current study is a combination investigation on macrocyclic and organometallic chemistry and it can provide some useful information on the design, preparation and properties of new kinds of metal ion-aromatic macrocyclic complexes.

## Experimental Section

### Materials and Methods

Unless otherwise specified, solvent of analytical grade were purchased directly from commercial sources and used without any further purification. The extended dialdehydes  $\text{H}_2\text{hpdd}$  and  $\text{H}_2\text{pdd}$  are prepared as the reported literature.<sup>3d</sup>

$^1\text{H}$  and  $^{13}\text{C}$  NMR spectra spectroscopic measurements were performed on a Bruker AM-500 NMR spectrometer, using TMS

(SiMe<sub>4</sub>) as an internal reference at room temperature. Elemental analyses were measured with a Perkin-Elmer 1400C analyzer. Infrared spectra (4000–400 cm<sup>-1</sup>) were collected on a Nicolet FT-IR 170X spectrophotometer at 25°C using KBr plates. Electrospray ionization mass spectra (ESI-MS) were recorded by a ThermoFisher Scientific LCQ Fleet mass spectrometer in a scan range of 100–2000 amu.

### Preparation of Metal Complexes

**Synthesis of 1a.** Zn(NO<sub>3</sub>)<sub>2</sub>·6H<sub>2</sub>O (0.033 g, 0.11 mmol) was dissolved in ethanol (10 mL) and added to a solution of H<sub>2</sub>hpdd (0.048 g, 0.10 mmol) in hot ethanol (20 mL). The mixture was refluxed for 10 min, and an ethanol (10 mL) solution of 1,3-propanediamine (0.009 g, 0.1 mmol) was added. The yellow-green solution was refluxed for additional 2 h, cooled to room temperature and filtered. The filtrate was concentrated to give **1a** in a yield of 70 % (0.044 g). <sup>1</sup>H NMR (500 MHz, CD<sub>3</sub>OD): δ 8.28–8.25 (m, 2H), 7.97 (s, 2H), 7.92 (s, 4H), 7.13–7.10 (m, 4H), 6.89–6.86 (m, 4H), 6.61 (d, *J* = 7.5 Hz, 4H), 3.96 (s, 8H), 3.92 (s, 8H), 3.52 (dd, *J* = 13.9 and 7.7 Hz, 8H), 0.92 (d, *J* = 6.9 Hz, 4H). *Anal.* Calc. for C<sub>53</sub>H<sub>50</sub>Cl<sub>4</sub>N<sub>8</sub>O<sub>12</sub>Zn<sub>2</sub>: C, 50.38; H, 3.99; N, 8.87 %. Found: C, 50.20; H, 3.90; N, 8.97 %. ESI-MS (positive mode, *m/z*): 1183.08 [M+CH<sub>3</sub>OH+H]<sup>+</sup>. Main FT-IR absorptions (KBr pellets, cm<sup>-1</sup>): 3434, 2927, 1639 (s, -CH=N), 1549, 1450, 1386, 1153, 763. Light yellow-green single crystals of the solvate complex **1a**·C<sub>2</sub>H<sub>5</sub>OH were grown from a mixture of ethanol/acetonitrile (*v/v* = 2:1) by slow evaporation in air at room temperature.

**Synthesis of 1b.** The synthetic process of **1b** is the same as that of **1a** except that H<sub>2</sub>pdd (0.047 g, 0.10 mmol) was used. Yield: 0.055 g (89 %). <sup>1</sup>H NMR (500 MHz, CD<sub>3</sub>CN): δ 8.24 (s, 1H), 8.18 (s, 1H), 7.99 (s, 1H), 7.97 (s, 1H), 7.41 (s, 1H), 7.36 (s, 2H), 7.32 (s, 1H), 7.29 (s, 2H), 7.26 (d, *J* = 4.6 Hz, 4H), 7.20 (d, *J* = 7.6 Hz, 1H), 7.15 (s, 3H), 7.01 (d, *J* = 7.3 Hz, 1H), 6.93 (s, 3H), 6.89 (s, 1H), 4.60 (d, *J* = 12.7 Hz, 2H), 4.20 (d, *J* = 12.2 Hz, 2H), 4.14–4.00 (m, 4H), 3.91 (d, *J* = 12.9 Hz, 1H), 3.72 (dd, *J* = 21.2 and 8.6 Hz, 4H), 3.62–3.50 (m, 4H), 3.46 (dd, *J* = 12.0 and 5.9 Hz, 4H), 3.37 (d, *J* = 12.8 Hz, 1H), 3.22 (d, *J* = 11.5 Hz, 2H), 2.60 (s, 1H), 2.47 (s, 3H). *Anal.* Calc. for C<sub>53</sub>H<sub>50</sub>Cl<sub>4</sub>N<sub>8</sub>O<sub>10</sub>Zn<sub>2</sub>: C, 51.68; H, 4.09; N, 9.10 %. Found: C, 51.80; H, 3.93; N, 9.01 %. ESI-MS (positive mode, *m/z*): 1151.48 [M+CH<sub>3</sub>OH+H]<sup>+</sup>. Main FT-IR absorptions (KBr pellets, cm<sup>-1</sup>): 3450, 2929, 1632 (s, -CH=N), 1555, 1453, 1385, 776, 700. Light yellow-green single crystals of the solvate complex **1b**·CH<sub>3</sub>OH were obtained from a mixture of methanol/acetonitrile (*v/v* = 10:1) by slow evaporation in air at room temperature.

**Synthesis of 2.** Anhydrous Pb(NO<sub>3</sub>)<sub>2</sub> (0.036 g, 0.11 mmol) was dissolved in methanol (15 mL) and added to a solution of H<sub>2</sub>hpdd (0.047 g, 0.10 mmol) in 15 mL hot methanol. After 10 min reflux, a 10 mL methanol solution of 1,3-propanediamine (0.008 g, 0.1 mmol) was added. The orange solution was refluxed for 2 h, cooled, filtered, and the volume was reduced to give the product in 40 % yield (0.029 g). <sup>1</sup>H NMR (500 MHz, CD<sub>3</sub>OD): δ 8.15 (s, 2H), 7.35 (d, *J* = 8.1 Hz, 2H), 7.05 (s, 2H), 6.94 (s, 2H), 6.87 (d, *J* = 7.9 Hz, 2H), 4.59 (s, 8H), 4.14 (dd, *J* = 21.3 and 12.1 Hz, 4H), 3.91 (d, *J* = 12.2 Hz, 2H), 3.82 (t, *J* = 6.8 Hz, 2H). *Anal.* Calc. for C<sub>27</sub>H<sub>27</sub>Cl<sub>2</sub>N<sub>3</sub>O<sub>4</sub>Pb: C, 44.08; H, 3.70; N, 5.71 %. Found: C, 44.20; H, 3.80; N, 5.82 %. Main FT-IR absorptions (KBr pellets, cm<sup>-1</sup>): 3451, 2933, 2863, 1634 (s, -CH=N), 1451, 1378, 1304, 760. Orange yellow crystals of complex **2** were

obtained from a mixture of methanol/acetonitrile (*v/v* = 8:1) by slow evaporation in air at room temperature.

**Synthesis of 3.** The synthetic process of **3** is the same as that of **2** except that H<sub>2</sub>pdd (0.046 g, 0.10 mmol) was used. Yield: 86 %, (0.065 g). Orange yellow crystals of complex **3** were obtained by slow evaporation of a mixture of methanol/acetonitrile solution (*v/v* = 1:1) in air at room temperature. <sup>1</sup>H NMR (500 MHz, CD<sub>3</sub>OD): δ 8.17 (s, 2H), 7.56 (d, *J* = 7.5 Hz, 2H), 7.48 (t, *J* = 7.5 Hz, 2H), 7.39 (dd, *J* = 11.1, 4.1 Hz, 1H), 7.07 (d, *J* = 2.0 Hz, 2H), 6.96 (d, *J* = 2.2 Hz, 2H), 4.25–4.11 (m, 4H), 3.98–3.86 (m, 4H), 3.45 (t, *J* = 7.0 Hz, 2H). *Anal.* Calc. for C<sub>54</sub>H<sub>52</sub>Cl<sub>4</sub>N<sub>8</sub>O<sub>10</sub>Pb<sub>2</sub>: C, 42.41; H, 3.43; N, 7.33 %. Found: C, 42.55; H, 3.49; N, 7.21 %. Main FT-IR absorptions (KBr pellets, cm<sup>-1</sup>): 3446, 2938, 2876, 1634 (s, -CH=N), 1545, 1446, 1378, 1305, 757.

**Synthesis of 4.** Dilute HNO<sub>3</sub> (0.05 mol/L) was added to a solution of **1b** (0.062 g, 0.049 mmol) in methanol (20 mL) till the pH value of mixture is *ca.* 3–4 at room temperature. Then the yellow green mixture was stirred for 2 h, filtered and concentrated to give complex **4** in a yield of 41 % (0.024 g). Yellow green crystals of complex **4** were obtained by slow evaporation of a mixture of methanol/acetonitrile solution (*v/v* = 8:1) in air at room temperature. <sup>1</sup>H NMR (500 MHz, CD<sub>3</sub>OD): δ 7.91 (s, 2H), 7.25–7.20 (m, 8H), 7.17 (d, *J* = 7.0 Hz, 2H), 7.13 (s, 4H), 7.07 (d, *J* = 7.6 Hz, 4H), 5.54 (s, 2H), 3.35 (s, 6H), 2.04 (s, 4H). *Anal.* Calc. for C<sub>54</sub>H<sub>58</sub>Cl<sub>4</sub>N<sub>2</sub>O<sub>12</sub>Zn<sub>2</sub>: C, 54.06; H, 4.87; N, 2.34 %. Found: C, 53.98; H, 4.75; N, 2.27 %. Main FT-IR absorptions (KBr pellets, cm<sup>-1</sup>): 3433, 2968, 2919, 2878, 1645 (s, -CH=O), 1544, 1456, 1210, 838, 556.

### X-Ray Data Collection and Structural Determination

Single-crystal samples of five compounds were covered with glue and mounted on glass fibers and then used for data collection. Crystallographic data were collected on a Bruker SMART 1K CCD diffractometer, using graphite mono-chromated Mo K $\alpha$  radiation ( $\lambda$  = 0.71073 Å). The crystal systems were determined by Laue symmetry and the space groups were assigned on the basis of systematic absences using XPREP. Absorption corrections were performed to all data and the structures were solved by direct methods and refined by full-matrix least-squares method on  $F_{obs}^2$  by using the SHELXTL-PC software package.<sup>7</sup> All non-H atoms were anisotropically refined and all hydrogen atoms were inserted in the calculated positions assigned fixed isotropic thermal parameters and allowed to ride on their respective parent atoms. The summary of the crystal data, experimental details and refinement results for five metal complexes is listed in Table 1, whereas selected bond distances and angles are given in Table SII. In addition, hydrogen-bonding parameters are tabulated in Table SII.

### Acknowledgment

This work was financially supported by the Major State Basic Research Development Programs (Nos. 2013CB922101 and 2011CB933300), the National Natural Science Foundation of China (No. 21171088), and the Natural Science Foundation of Jiangsu Province (Grant BK20130054).

### Notes

<sup>a</sup> State Key Laboratory of Coordination Chemistry, Nanjing National Laboratory of Microstructures, School of Chemistry and Chemical Engineering, Nanjing University, Nanjing 210093, P.R. China. Fax: 86 25 8331 4502; Tel: 86 25 8368 6526; E-mail: whuang@nju.edu.cn

<sup>b</sup> College of Sciences, Nanjing Tech University, Nanjing, 210009, P. R. China

† Electronic Supplementary Information (ESI) available: Selected bond distances (Å) and angles (°), hydrogen bonding parameters, FT-IR spectra and perspective view of the packing structures for related complexes. CCDC nos. 955028–955031 and 1009728 contain the supplementary crystallographic data for five complexes in this work. These data could be acquired free of charge via [www.ccdc.cam.ac.uk/conts/retrieving.html](http://www.ccdc.cam.ac.uk/conts/retrieving.html) (or from the Cambridge Crystallographic Data Centre, 12 Union Road, Cambridge CB21EZ, UK; fax: [+44]1223-336-033; or deposit [@ccdc.cam.ac.uk](mailto:@ccdc.cam.ac.uk)).

## References

- (a) J. M. Lehn, *Supramolecular Chemistry. Concepts and Perspectives*; VCH: Weinheim, Germany, 1995; (b) T. Dziembowska, N. Guskos, J. Typek, R. Szymczak, V. Likodimos, S. Glenis, C. L. Lin, M. Wabia, E. Jagodzinska and E. Fabrycy, *Mater. Res. Bull.*, 1999, **34**, 943-954; (c) J. C. Roder, F. Meyer and E. Kaifer, *Angew. Chem., Int. Ed.*, 2002, **41**, 2304-2306; (d) A. P. Nelson and S. G. DiMugno, *J. Am. Chem. Soc.*, 2000, **122**, 8569-8570; (e) S. R. Korupolu, N. Mangayarkarasi, S. Ameerunisha, E. J. Valente and P. S. Zacharias, *J. Chem. Soc., Dalton Trans.*, 2000, 2845-2852; (f) A. Bianchi, K. Bowman-James and E. Garcia-Espana, *Supramolecular Chemistry of Anions*; Wiley-VCH, New York, 1997; (g) S. J. Lippard and J. M. Berg, *Principles of Bioinorganic Chemistry*; University Science Books: Mill Valley, CA, 1994; (h) E. I. Solomon, U. M. Sundaram and T. E. Machonkin, *Chem. Rev.*, 1996, **96**, 2563-2605.
- (a) N. E. Borisova, M. D. Reshetova and Y. A. Ustynyuk, *Chem. Rev.*, 2007, **107**, 46-79; (b) P. A. Vigato, S. Tamburini and L. Bertolo, *Coord. Chem. Rev.*, 2007, **251**, 1311-1492; (c) W. Radecka-Paryzek, V. Patroniak and J. Lisowski, *Coord. Chem. Rev.*, 2005, **249**, 2156-2175; (d) P. A. Vigato and S. Tamburini, *Coord. Chem. Rev.*, 2004, **248**, 1717-2128.
- (a) W. Huang, H. B. Zhu and S. H. Gou, *Coord. Chem. Rev.*, 2006, **250**, 414-423; (b) J. C. Jiang, Z. L. Chu, W. Huang, G. Wang and X. Z. You, *Inorg. Chem.*, 2010, **49**, 5897-5911; (c) H. Q. Chen, K. Zhang, C. Jin and W. Huang, *Dalton Trans.*, 2014, **43**, 8486-8492; (d) K. Zhang, C. Jin, H. Q. Chen, G. Yin and W. Huang, *Chem. Asian J.*, 2014. DOI: 10.1002/asia.201402357R1.
- (a) H. R. Chang, S. K. Larsen, P. D. W. Boyd, C. G. Pierpont and D. N. Hendrickson, *J. Am. Chem. Soc.*, 1988, **110**, 4565-4576; (b) M. Tadokoro, H. Sakiyama, N. Matsumoto, H. Okawa and S. Kida, *Bull. Chem. Soc. Jpn.*, 1990, **63**, 3337-3339; (c) B. Dutta, B. Adhikary, P. Bag, U. Florke and K. Nag, *J. Chem. Soc., Dalton Trans.*, 2002, 2760-2767; (d) A. J. Atkins, A. J. Blake and M. Schroder, *J. Chem. Soc., Chem. Commun.*, 1993, 353-355; (e) D. Black, A. J. Blake, R. L. Finn, L. F. Lindoy, A. Nezhadali, G. Rougnaghi, P. A. Tasker and M. Schroder, *Chem. Commun.*, 2002, 340-341; (f) B. Liu, H. Zhou, Z. Q. Pan, X. L. Hu and L. Chen, *Acta Crystallogr.*, 2005, **E61**, m1295-m1297; (g) B. F. Hoskins and G. A. Williams, *Aust. J. Chem.*, 1975, **28**, 2607-2614; (h) B. Dutta, P. Bag, U. Florke and K. Nag, *Inorg. Chem.*, 2005, **44**, 147-157; (i) A. C. Raimondi, P. B. Hitchcock, G. F. Leigh and F. S. Nunes, *J. Chem. Cryst.*, 2004, **34**, 83-87; (j) A. Cucos, G. Marinescu, Z. Zak, N. Stanica and M. Andruh, *Rev. Roum. Chim.*, 2002, **47**, 989-995.
- A. W. Addison, T. N. Rao, J. Reedijk, J. Van Rijn and G. C. Verschoor, *J. Chem. Soc., Dalton Trans.*, 1984, 1349-1356.
- (a) T. J. Mooibroek, P. Gamez and J. Reedijk, *CrystEngComm*, 2008, **10**, 1501-1515; (b) H. Schmidbaur and A. Schier, *Organometallics*, 2008, **27**, 2361-2395; (c) E. R. T. Tiekink and J. Zukerman-Schpector, *Aust. J. Chem.*, 2010, **63**, 535-543; (d) M. Di Vaira, F. Mani and P. Stoppioni, *J. Chem. Soc., Dalton Trans.*, 1998, 3209-3214; (e) M. Di Vaira, M. Guerra, F. Mani and P. Stoppioni, *J. Chem. Soc., Dalton Trans.*, 1996, 1173-1179; (f) F. T. Edelmann, J.-K. F. Buijink, S. A. Brooker, R. Herbst-Irmer, U. Kilimann and F. M. Bohnen, *Inorg. Chem.*, 2000, **39**, 6134-6135; (g) J. P. H. Charmant, M. F. Haddow, F. E. Hahn, D. Heitmann, R. Frohlich, S. M. Mansell, C. A. Russell and D. F. Wass, *Dalton Trans.*, 2008, **43**, 6055-6059; (h) D. J. Teff, J. C. Huffman and K. G. Caulton, *Inorg. Chem.*, 1997, **36**, 4372-4380; (i) W. A. Merrill, R. J. Wright, C. S. Stanciu, M. M. Olmstead, J. C. Fettinger and P. P. Power, *Inorg. Chem.*, 2010, **49**, 7097-7105; (j) S. Hino, M. Brynda, A. D. Phillips and P. P. Power, *Angew. Chem., Int. Ed.*, 2004, **43**, 2655-2658; (k) M. C. Kuchta and G. Parkin, *New J. Chem.*, 1998, **22**, 523-530; (l) F. E. Hahn, D. Heitmann and T. Pape, *Eur. J. Inorg. Chem.*, 2008, **7**, 1039-1041; (m) A. G. Gash, P. F. Rodesiler and E. L. Amma, *Inorg. Chem.*, 1974, **13**, 2429-2434; (n) E. A. H. Griffith and E. L. Amma, *J. Am. Chem. Soc.*, 1974, **96**, 743-749.
- Sheldrick, G. M. SHELXTL (Version 6.10). Software Reference Manual; Madison, Wisconsin (USA): Bruker AXS, Inc.: 2000.

**Table 1.** Crystal Data and Structural Refinements for Compounds 1-4.

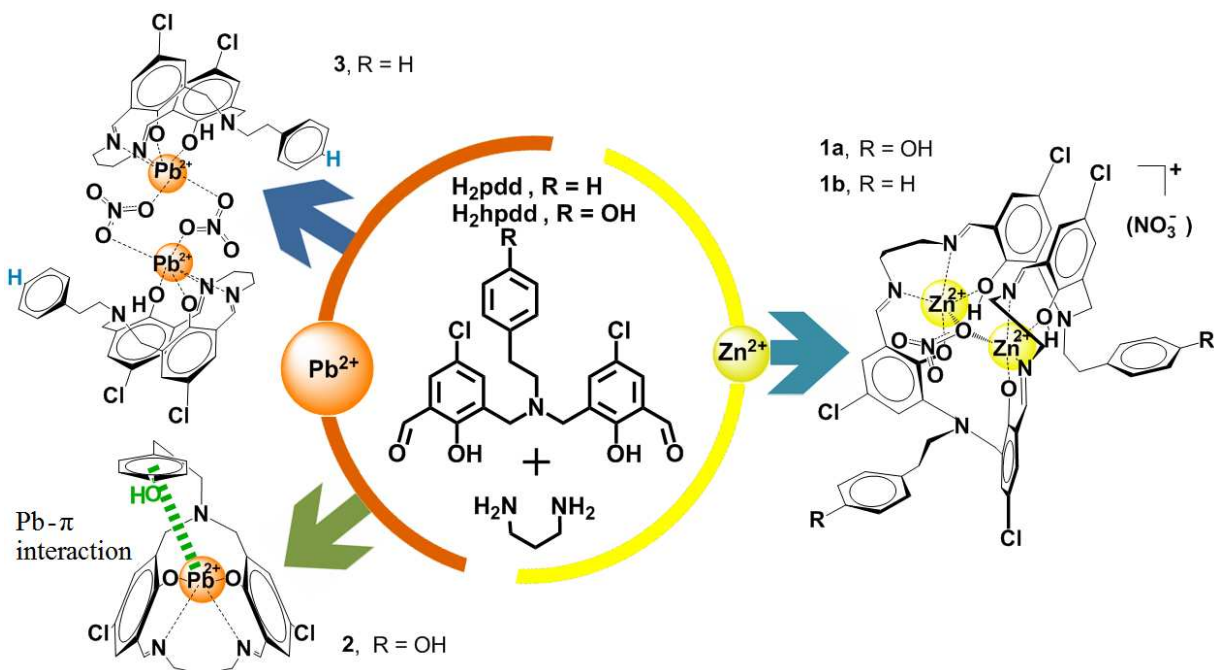
Complex	<b>1a</b> -C <sub>2</sub> H <sub>5</sub> OH	<b>1b</b> -CH <sub>3</sub> OH	<b>2</b>	<b>3</b>	<b>4</b>
Empirical formula	C <sub>56</sub> H <sub>58</sub> Cl <sub>4</sub> N <sub>8</sub> O <sub>13</sub> Zn <sub>2</sub>	C <sub>55</sub> H <sub>56</sub> Cl <sub>4</sub> N <sub>8</sub> O <sub>11</sub> Zn <sub>2</sub>	C <sub>27</sub> H <sub>25</sub> Cl <sub>2</sub> N <sub>3</sub> O <sub>3</sub> Pb	C <sub>27</sub> H <sub>26</sub> Cl <sub>2</sub> N <sub>4</sub> O <sub>5</sub> Pb	C <sub>54</sub> H <sub>58</sub> Cl <sub>4</sub> N <sub>2</sub> O <sub>12</sub> Zn <sub>2</sub>
Formula weight	1323.64	1277.62	717.59	764.61	1199.60
Temperature / K	291(2)	291(2)	291(2)	291(2)	291(2)
Wavelength / Å	0.71073	0.71073	0.71073	0.71073	0.71073
Crystal Size (mm)	0.12×0.12×0.10	0.14×0.14×0.10	0.10×0.08×0.08	0.12×0.10×0.08	0.10×0.10×0.10
Crystal system	Triclinic	Triclinic	Triclinic	Monoclinic	Monoclinic
Space group	<i>P</i> $\bar{1}$	<i>P</i> $\bar{1}$	<i>P</i> $\bar{1}$	<i>C</i> 2/ <i>m</i>	<i>P</i> 2 <sub>1</sub> / <i>c</i>
<i>a</i> / Å	13.244(3)	13.689(9)	10.404(3)	20.254(8)	11.255(7)
<i>b</i> / Å	13.505(3)	14.944(10)	10.422(3)	10.682(3)	15.508(9)
<i>c</i> / Å	17.957(4)	15.540(10)	13.660(4)	13.612(4)	17.377(9)
$\alpha$ / °	89.565(3)	105.066(10)	98.637(5)	90	90
$\beta$ / °	72.204(2)	107.277(10)	102.317(5)	98.762(8)	112.50(3)
$\gamma$ / °	72.003(3)	93.069(10)	99.253(4)	90	90
<i>V</i> / Å <sup>3</sup>	2895.1(11)	2901.5(3)	1401.9(7)	2910.6(16)	2802(3)
<i>Z</i> / <i>D</i> <sub>calcd</sub> (g / cm <sup>3</sup> )	2 / 1.518	2 / 1.462	2 / 1.700	4 / 1.745	2 / 1.422
<i>F</i> (000)	1364	1316	696	1488	1240
$\mu$ / mm <sup>-1</sup>	1.084	1.076	6.240	6.023	1.108
<i>h</i> <sub>min</sub> / <i>h</i> <sub>max</sub>	-12 / 15	-16 / 10	-12 / 10	-24 / 18	-13 / 12
<i>k</i> <sub>min</sub> / <i>k</i> <sub>max</sub>	-16 / 16	-17 / 17	-12 / 11	-12 / 11	-18 / 18
<i>l</i> <sub>min</sub> / <i>l</i> <sub>max</sub>	-21 / 21	-13 / 18	-13 / 16	-16 / 16	-20 / 19
Data / parameters	10081 / 748	10158 / 721	4919 / 334	2696 / 194	4843 / 337
<i>R</i> <sub>1</sub> , <i>wR</i> <sub>2</sub> [ <i>I</i> > 2 $\sigma$ ( <i>I</i> )] <sup>a</sup>	<i>R</i> <sub>1</sub> = 0.0469 <i>wR</i> <sub>2</sub> = 0.1277	<i>R</i> <sub>1</sub> = 0.0794 <i>wR</i> <sub>2</sub> = 0.1966	<i>R</i> <sub>1</sub> = 0.0372 <i>wR</i> <sub>2</sub> = 0.0802	<i>R</i> <sub>1</sub> = 0.0691 <i>wR</i> <sub>2</sub> = 0.1626	<i>R</i> <sub>1</sub> = 0.0761 <i>wR</i> <sub>2</sub> = 0.1358
<i>R</i> <sub>1</sub> , <i>wR</i> <sub>2</sub> (all data) <sup>b</sup>	<i>R</i> <sub>1</sub> = 0.0763 <i>wR</i> <sub>2</sub> = 0.1397	<i>R</i> <sub>1</sub> = 0.1058 <i>wR</i> <sub>2</sub> = 0.2098	<i>R</i> <sub>1</sub> = 0.0526 <i>wR</i> <sub>2</sub> = 0.0836	<i>R</i> <sub>1</sub> = 0.0777 <i>wR</i> <sub>2</sub> = 0.1659	<i>R</i> <sub>1</sub> = 0.2268 <i>wR</i> <sub>2</sub> = 0.1776
<i>S</i>	1.00	0.98	0.92	1.08	0.88
Max/min $\Delta\rho$ /e Å <sup>-3</sup>	0.94 / -0.47	3.27 / -0.52	1.00 / -1.06	4.49 / -3.03	0.39 / -0.72

<sup>a</sup> *R*<sub>1</sub> =  $\sum||F_o| - |F_c|| / \sum|F_o|$ , <sup>b</sup> *wR*<sub>2</sub> =  $[\sum[w(F_o^2 - F_c^2)^2] / \sum w(F_o^2)^2]^{1/2}$

## Graphical Abstract

Distinguishable Zn(II) and Pb(II) template effects on forming pendant-armed Schiff-base macrocyclic complexes including a remarkable Pb(II)- $\pi$  macrocyclic complex

Kun Zhang, Jiao Geng, Chao Jin and Wei Huang



36-Membered [2+2] dinuclear  $\text{Zn}(\text{II})$  and  $\text{Pb}(\text{II})$  Schiff-base macrocyclic complexes have been described, including a unique intramolecular  $\eta^3$ -coordinated  $\text{Pb}(\text{II})-\pi$  macrocyclic complex obtained under ambient condition.